C. R. Palevol 15 (2016) 968–977

Contents lists available at ScienceDirect

Comptes Rendus Palevol

www.sciencedirect.com

General Palaeontology, Systematics and Evolution (Vertebrate Palaeontology)

Photogrammetry for 3D digitizing bones of mounted skeletons: Potential and limits

Apport de la photogrammétrie à la numérisation 3D d'os de spécimens montés : potentiel et limites

Marine Fau [a,*], Raphaël Cornette [b], Alexandra Houssaye [a]

[a] *UMR 7179 CNRS/Muséum national d'histoire naturelle, département Écologie et Gestion de la biodiversité, 57, rue Cuvier, CP 55, 75005 Paris, France*
[b] *Institut de systématique, evolution, biodiversité, ISYEB, UMR 7205, CNRS, MNHN, UPMC, EPHE, Muséum national d'histoire naturelle, Sorbonne universités, 57, rue Cuvier, 75005 Paris, France*

ARTICLE INFO

Article history:
Received 25 January 2016
Accepted after revision 8 August 2016
Available online 16 September 2016

Handled by Michel Laurin

Keywords:
Photogrammetry
Mounted skeletons
Paleontology
3D
Digitization
Agisoft photoscan
VisualSFM

ABSTRACT

Since the late 20th century, new technologies have provided powerful ways to digitize biological structures in three dimensions (3D). Among those, photogrammetry is a low cost and non-destructive method, which has become increasingly used since the development of the digital camera. Recent studies have demonstrated that reconstructions of isolated elements can be of as high quality as those obtained with laser scanners. Here, we wanted to test the performance of photogrammetry for the quantitative analysis of mounted specimens in museum exhibitions. Indeed, access to material can be an issue in comparative anatomy and, especially, in paleontology. This is notably the case for large, impressive specimens. We performed reconstructions based on acquisitions done under various conditions and also tested the reconstruction performance of two software programs. The resulting 3D models were then compared to a reference object corresponding to the bone of interest digitized with a cutting-edge surface scanner. Our results show that photogrammetry enables quality reconstruction of the almost entire surface of the mounted bone of interest. Photogrammetry thus appears a reliable method perfectly suited to study large specimens exposed in museum gallery.

Mots clés :
Photogrammétrie
Squelettes montés
Paléontologie
3D
Digitalisation
Agisoft photoscan
VisualSFM

RÉSUMÉ

Depuis la fin du XX^{e} siècle, de nouvelles technologies ont fourni des outils puissants permettant de numériser des structures biologiques en trois dimensions (3D). Parmi ceux-ci, la photogrammétrie est une méthode bon marché et non destructive, qui a connu un essor avec le développement des appareils photonumériques. Des études récentes ont montré que les reconstructions par photogrammétrie d'éléments isolés peuvent être d'aussi bonne qualité que celles obtenues avec des scanners surfaciques. Ici, nous avons testé les performances de la photogrammétrie pour l'analyse quantitative de spécimens exposés dans des musées. En effet, l'accès au matériel peut être problématique en anatomie comparée ou en paléontologie ; c'est notamment le cas pour les spécimens de grande taille. Plusieurs reconstructions ont été faites avec des photographies prises dans des conditions différentes, et en utilisant

* Corresponding author.
E-mail address: marine.fau@hotmail.fr (M. Fau).

http://dx.doi.org/10.1016/j.crpv.2016.08.003
1631-0683/

deux logiciels différents, afin de tester leurs prestations. Les modèles 3D obtenus ont été alors comparés à un objet de référence : l'os étudié, numérisé avec un scanner surfacique de pointe. Les résultats montrent que la photogrammétrie permet une reconstruction de bonne qualité de pratiquement toute la surface de l'os étudié. La photogrammétrie apparaît donc comme une méthode fiable et parfaitement adaptée pour l'étude des spécimens de grande taille exposés dans des galeries de musées.

1. Introduction

Nowadays, a small revolution is occurring in paleontology, thanks to progress in computer and digital sciences: the emergence of "virtual paleontology" (Cunningham et al., 2014; Rahman and Smith, 2014). Since the late 20th century, new technology has provided powerful ways to better visualize/image fossils and, especially, non-destructive digitizing techniques. For example, synchrotron X-ray micro-tomography (Laloy et al., 2013; Pradel et al., 2009; Rücklin et al., 2014) enables us to see through rock and to have access to internal structures. Conversely, three dimension (3D) surface analyses are generally acquired with surface scanners (e.g., Clarac et al., 2015; Falkingham, 2012) or photogrammetry (e.g., Belvedere et al., 2013; Brassey et al., 2015; Castanera et al., 2013; Falkingham, 2012; Petti et al., 2008). Photogrammetry is a method for reconstructing an object in 3D from photographs. It can be performed with either terrestrial (close-range) or aerial photographs. Among all 3D-digitizating techniques, photogrammetry is one of the easiest and less expensive (Cunningham et al., 2014), because it only requires a camera and specific software.

Photogrammetry relies on optics and projective geometry principles (e.g., human stereoscopic vision: allowing us to see in 3D by observation of an object from two different points of view). The first trial/application of photogrammetric reconstruction was performed by A. Laussedat in 1849, in Paris, but it was only in the 1900s that photogrammetry started to be used on a large scale, thanks to the development of digital technology (Jiang et al., 2008). Photogrammetry is already commonly used in some research fields like geology, for monitoring earth deformation from aerial or satellite photographs (e.g., Lane et al., 2000; Mora et al., 2003; Wolf and Dewin, 2000), in archeology to improve *in situ* topological or taphonomic data acquisition (De Reu et al., 2013, 2014), or for surveys of the cultural heritage (e.g., Guarnieri et al., 2004; Salonia et al., 2007, 2009). In paleontology, photogrammetry has only been used for a few years (Breithaupt and Matthews, 2001; Breithaupt et al., 2001, 2004; Matthews and Breithaupt, 2001), but 3D digitizing of both specimens and surfaces of excavation, in particular for ichnofossils, is increasingly used (e.g., Belvedere et al., 2013; Brassey et al., 2015; Castanera et al., 2013; Falkingham, 2012; Petti et al., 2008). There is no theoretical limitation of specimen size for using photogrammetry. Various kinds of specimens can be digitized, such as arthropods, vegetal remains (Falkingham, 2012), ichnofossils (e.g., Castanera et al., 2013) and naturally bones and teeth (Falkingham, 2013).

Multi-image based 3D reconstructions are suitable for a quantitative approach (e.g., Brassey et al., 2015; Hutchinson et al., 2005; Koutsoudis et al., 2013). Recent studies showed that photogrammetry can produce 3D reconstructions with similar or even better resolution, than some laser scanners (Falkingham, 2012; Petti et al., 2008; Remondino et al., 2010). Access to large specimens can be complicated. For example, most of the biggest fossil specimens are exposed in museums, since they are much appreciated by the public. Large vertebrate specimens are generally exhibited as mounted skeletons and so not easily accessible for scientific studies (notably for dismounting and transport issues). For this reason, photogrammetry appears a particularly well-adapted method to digitize bones of large mounted specimens. In addition to the difficulty in accessing the entire surface of bones because of mounting (e.g., contact between bones, braces), museum galleries also usually show a problematic lack of light.

The present contribution proposes a test of the possibilities offered by photogrammetry in this context and of its limits. It focuses on the mounted specimen of a giant fossil ratite bird to estimate the performance of photogrammetry in museum gallery conditions through the use of two different photogrammetric processing pieces of software, and compares the 3D models obtained to those acquired with a cutting edge surface-scanner.

2. Materials and Methods

2.1. Biological material

The specimen of an extinct giant ratite bird, *Aepyornis maximus* Saint Hilaire, 1851 (Aves, Paleognathae, Aepyornithidae; specimen MNHN.F.MAD 8901) was chosen (Fig. 1). It comprises mounted hind limbs and pelvis. The specimen was available in the paleontological collections of the "Muséum national d'histoire naturelle" of Paris (MNHN), and exposed in a rather poorly-illuminated room mimicking the luminosity of some museum galleries. The specimen was chosen because it was easily accessible, and available for disassembling (for comparative surface scanning). The present study focuses on the right femur of this specimen, which is about 42 cm long (from the top of the proximal epiphysis to the distal epiphysis). A single bone was selected in order to control variations relying on changes of parameters of interest (light, photoflash and parameters of the SLR [Single-lens reflex] camera) and remove variations specific to the specimen used and/or the bone itself (color or texture). Indeed, surface-based

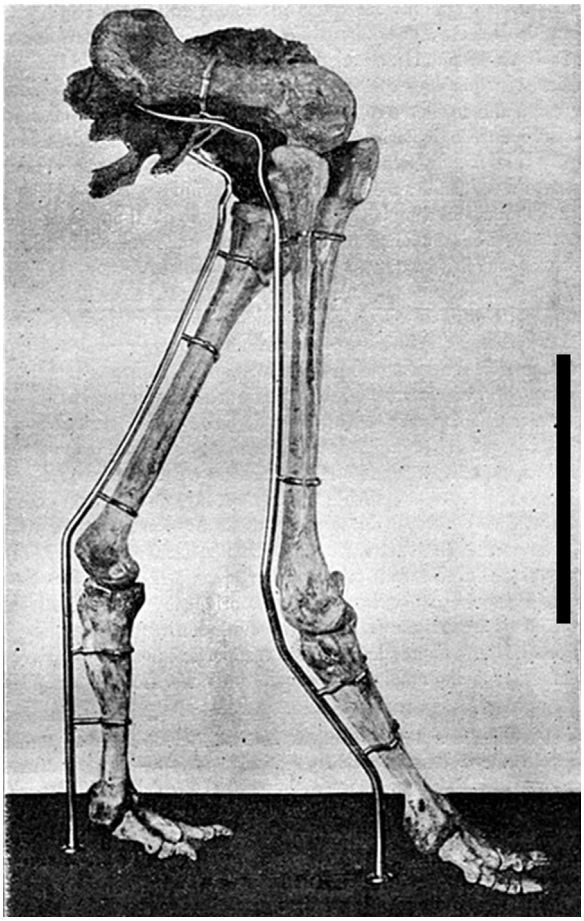

Fig. 1. Picture of the specimen of *Aepyornis maximus* (MNHN.F.MAD 8901) used in this study, in its original position. Profil view, modified from Grandidier (1903). Scale bar: 40 cm.
Fig. 1. Photographie du spécimen d'*Aepyornis maximus* (MNHN.F.MAD 8901) utilisé dans cette étude, en position originale. Vue de profil, modifiée d'après Grandidier (1903). Barre d'échelle : 40 cm.

acquisition methods, such as photogrammetry, are highly sensitive to the surface color and texture (Koutsoudis et al., 2013).

2.2. Devices for acquisition and analysis

Photography was done using a Pentax K10D Digital SLR Camera (10.2 effective megapixels, focal length: 18–55 mm). After the photographs, the specimen was disassemble and the isolated right femur was scanned with a branded light-fringe scanner Breukmann Stereoscan 3D (AICON 3D Systems Gmb, Biberweg 30 C, 38114, Braunschweig, Germany). Given the high resolution and the high quality of this surface scanner (scope: 720 mm, resolution: 22 μm), and its regular use for quantitative studies (e.g., Bonneau et al., 2012; Clarac et al., 2015; Fabre et al., 2015; Polly et al., 2013), the 3D model obtained was then considered the reference 3D model, or reference object (RO).

Two software programs were used for the 3D reconstructions:

- the open source VisualSFM (Wu, 2011; Wu et al., 2011);
- the commercial Agisoft PhotoScan (© 2014 Agisoft LLC, 27 Gzhatskaya st., St. Petersburg, Russia).

Open source software programs are characterized by the possibility to study and modify the source code. Conversely, in a commercial or proprietary software, the source code is not available and not editable. According to Bartoš et al. (2014), VisualSFM is the best open source software available for the moment in terms of reconstruction quality (point cloud density and deviation from the reference object). Moreover, this software is used by paleontologists (e.g., Brassey et al., 2015; Castanera et al., 2013). Agisoft PhotoScan, also recently used in paleontology (e.g., Belvedere et al., 2013), is considered the most efficient (L. Cazes, pers. comm.) and most user-friendly 3D reconstruction image-based software for the moment. Both software programs exploit the computer vision algorithm Structure-From-Motion (SFM) coupled with another complementary algorithm: Dense Multi-View 3D Reconstruction (DMVR). Two different DMVR algorithms can be installed in VisualSFM: Clustering Views for Multi-view Stereo (CVMS, used here) or Patch-based Mutli View Stereo (PMVS) (Mallison and Wings, 2014).

The SFM algorithm creates a point cloud in 3D from photographs taken at different viewpoints, without order or number constraint (minimal number is 2). It identifies corresponding features between each pair of images and then calculates the camera position parameters. The point cloud obtained through this algorithm does not display a sufficient density to generate a surface (polygonal 3D mesh), so a second 3D reconstruction ("dense reconstruction") using the CVMS, PMVS or another DMVR algorithm, is necessary. The CVMS/PMVS algorithm decomposes the image set into a set of image clusters of manageable size, and then puts all clusters together, which provides more details than if the whole image set were treated at a time (Furukawa and Ponce, 2010). In Agisoft Photoscan, the complementary algorithm (DMVR) seeks correspondence between each pixel of the photographs, and that particularity leads Photoscan to offer several levels of detail (lowest, low, medium, high, and ultra-high) to the user at the beginning of each step of the reconstruction. With the Ultra-high option, Photoscan processes with the original resolution of the photographs, and at each of the following steps, the resolution is downscaled by a factor of 4 (pixel number divided by 2, in length and width). Here we always used the lowest option, because it was already of sufficient quality, and it was fairer to compare the lowest results that can be obtained in both programs. Moreover, because the two programs are using different algorithms and because Photoscan is a proprietary software, it would have been very difficult or even impossible to get comparable results with optimized parameters (dense reconstruction parameters are accessible through the graphical user interface in Photoscan, and through a file named nv.ini in VisualSFM).

2.3. Data acquisition

The first step was taking pictures of the right femur. Thirteen sets of photographs were taken (Table 1) in order

Table 1
Description of each set of photographs used for the 3D reconstruction. Light condition refers to the use or not of the additional artificial light (AF) of the room. Photoflash: number of photographs taken with photoflash. Shooting time (in minutes) is only indicative, as sets with photoflash were taken independently from the rest of the set and added after to the set, the time is bigger (time for taking photographs with photoflash added to the time for the original set [S1, S5, S6]).
Tableau 1
Description des séries de photographies utilisées pour les reconstructions 3D. Les conditions lumineuses correspondent à l'allumage du système lumineux artificiel de la pièce (AF). *Photoflash* : nombre de photographies prises avec utilisation du flash. *Shooting time* (en minutes) : durée indicative de chaque séance photo. Les photographies avec flash ayant été prises lors de séances supplémentaires, les durées de ces séances ont été ajoutées aux durées des séances initiales (S1, S5, et S6).

Set number	Light condition	Photoflash	ISO	Total number of pictures	Shooting time
S1	AF	–	200	245	45
S2	–	–	1600	245	45
S3	AF	–	1600	245	30
S4	AF	–	1600	245	30
S5	–	–	1600	245	30
S6	–	–	1600	245	30
S7	AF	–	800	245	30
S8	–	–	800	245	40
SF1	AF	40	200	245	55
SF5	–	40	1600	245	40
SF6	–	40	1600	285	40

to test repeatability in different conditions and the impact of lighting conditions, camera's sensitivity: ISO, and of the use of the photoflash. The number of photographs in each set was fixed at 245 pictures in order not to introduce more variation factors than those tested here. Two hundred and forty-five photographs were enough to cover the entire specimen and zoom in more problematic dark or hardly accessible areas. Because of the specimen size (about 1.5 m high), no turning table could be used and the operator (M.F.) had to turn around it to take pictures, and to use a stool to take cons-diving pictures. The picture acquisition was always performed similarly and by the same operator. All current photogrammetric pieces of software calculate the distance between the camera and the specimen, allowing the users to walk around and take photographs at different distances from the specimen. Eight sets were taken without using the photoflash, four of which (S4, S5, S6, S8) were taken with only the natural light of the room, and the four other sets (S1, S2, S3, S7) with the addition of artificial light in the room. Two sets (SF1, SF5) were made by randomly replacing 40 pictures of the original sets (S1, S5) by 40 pictures taken using the photoflash. Another set (SF6) was obtained by adding the 40 pictures taken with the photoflash to the original set (S6); it is thus the only set with more than 245 pictures. The last two sets (Sext1, Sext2) were taken outside, on the bone once unmounted, on a sunny afternoon to perform photogrammetry on optimal light conditions, i.e. with naturally bright lighting conditions. Two sets were performed because of the necessity to put the femur on a support (a stool), and of the resulting acquisition of only incomplete (one side) data. Combining photographs from two such sets in order to obtain a complete bone requires to configure (and not only use with default parameters) photogrammetric software. Here, the objective was to use each software equally with its default parameters. That is why the two sets were treated separately.

The focal length was fixed at 35 mm, and neither the shutter speed nor the diaphragm was fixed, but the automatic mode was preferred. Indeed, the acquisition was performed by walking around the specimen, this means that the light was not homogeneous around the specimen, so that exposure parameters needed to be changed (Mallison and Wings, 2014). Moreover, all current photogrammetric pieces of software take these parameters into account during the reconstruction process. Only the camera's sensitivity (ISO) was modified, because of the assumed important role it might play to find an equilibrium between unsharpness (at low ISO value) and high image noise (or "grain", at high ISO value). This factor was tested by taking two picture sets at 200 ISO (S7, S8), two sets at 800 ISO (S1, SF1) and the remaining nine sets at 1600 ISO (see Table 1).

Two 3D reconstructions were performed for each set of photographs, one with each of the two programs. Assuming that the default parameters are supposed to be the most versatile, except the choice of the level of detail in Photoscan, both programs have only been used with their default parameters. The "dense reconstruction" step (i.e. 3D point cloud as dense as possible) was performed on Photoscan and on VisualSFM with the CMVS tool chain. It was then cleaned, when necessary, in Geomagic Studio 2012 (Geomagic Worldwide Headquarters 430 Davis drive, Marisville, NC), to remove non-desired additional objects (e.g., parts of the surrounding bones), artefacts, and noise(s). Then, the point cloud was transformed into a mesh (i.e. polygonal 3D object made of vertices, edges and faces.) with Geomagic Studio. Because this option is present in Photoscan, but absent in VisualSFM, Geomagic Studio was used for the mesh building in order to use the same mesh generator algorithm for each 3D model. Finally, a surface (3D polygon mesh) was generated and a second cleaning step was done, after which the 3D object was ready for analysis.

2.4. Quantitative analyses

The RO was considered an almost exact replica of the real femur and thus used as a reference for estimating the quality of the photogrammetric 3D models. The latter were

aligned with the RO, using a best-fit algorithm (in Geomagic Studio) to ensure they were properly superimposed. Up-to-the scale is first made by the operator; then the software calculates the rotation for the best possible alignment. Various quantitative parameters relative to the 3D objects obtained were listed: (1) area of the reconstructed surface (in mm^2) (Area); (2) percentage of the reconstructed surface (PRS), i.e. area of the reconstructed surface as compared to the RO. The deviation analysis corresponds to the distance between one point of the 3D model's surface and the corresponding point of the RO's surface (Warne, 2015). The deviation analysis was performed in order to determine if the 3D models were a faithful representation of the reality. Surface comparison between the 3D photogrammetric models and the RO, provided four quantitative parameters; (3) maximum deviation (DevM), i.e. the maximum distance between the two surfaces (outlier); (4) mean positive deviation (DevP) (average distance between the two surfaces when the compared surface is above the reference surface); (5) mean negative deviation (DevN) (average distance between the two surfaces when the compared surface is below the reference surface); (6) the standard deviation of the mean deviation distance (ST). Parameters relative to the reconstruction process were also added: (7) number of photographs used for the "dense reconstruction" (NB) (VisualSFM, contrary to Photoscan, does not always use all loaded pictures for the "dense reconstruction" step); (8) face number (number of triangles composing the surface) (NF); (9) point number before any cleaning step (NBC); (10) point number after cleaning, equals the number of points of the final 3D model (NAC); (11) approximate cleaning time, in minutes (CT); and (12) approximate "dense reconstruction" time (RT).

Qualitative parameters were also listed: (1) the lighting conditions (artificial light added or not, or outdoor); (2) the ISO value (200, 800 or 1600); (3) the addition of photographs taken with the photoflash (always 40 photographs when added) (See Appendix 1).

Statistical tests (Shapiro test to assure normal distribution; Student test or *t*-test to compare two means; and Fisher test or F-test to assure that samples have the same variance) and a Principal Component Analysis (PCA, to resume the whole information and show the impact of the various parameters on the distribution of the reconstructed objects) were performed using the statistical software R (R Core Team, 2014). All quantitative data were log10-transformed before statistical analyses were performed and the normal distribution of each quantitative parameters was checked.

3. Results

3.1. Surface reconstruction

Because the two outdoor sets (Ext1, Ext2) were taken in very distinct conditions, we excluded these two sets when calculating the mean PRS of each software. There is a strong difference in the percentage of surface recovered between the two software. Indeed, VisualSFM reproduces much less surface than Photoscan (mean PRS = 59.4% *versus* 89.2%) (Fig. 2). A Student test confirms that the difference in mean PRS values between the two software is significant ($P < 0.001$). Likewise, VisualSFM found less matched cameras than Photoscan during the "dense reconstruction" step (mean NB = 239.5 *versus* 245 in Photoscan). VisualSFM clearly does not enable to reconstruct most of the femur, in contrary to Photoscan, which reproduces almost the whole femur surface, except naturally areas that are in contact with metal braces (caused by mounting) or other bones. For some areas that are not in contact but very close to other bones (here the pelvis) or to braces, the surface is not always recovered, even with Photoscan.

The PRS values for the two outdoor sets are 61.0% (Ext1) and 62.5% (Ext2) with VisualSFM; 88.6% (Ext1) and 81.5% (Ext2) with Photoscan. We cannot compare the PRS of the outdoor sets to the sets taken previously when the

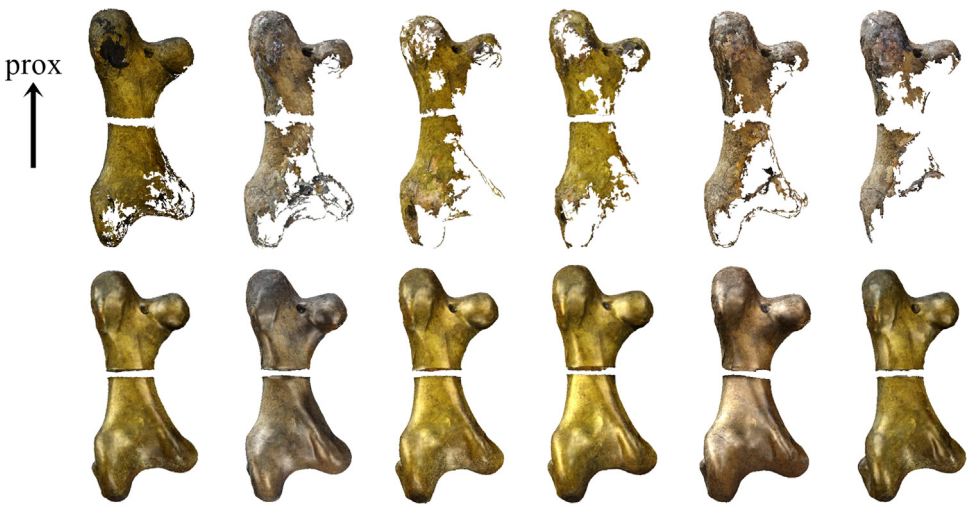

Fig. 2. Series of 3D reconstructions. Top line (a): reconstructions with VisualSFM; Bottom line (b): reconstructions with Photoscan. The sets from left to right: S1, S2, S3, S4, S5, S6. The arrow indicates the orientation of the proximal epiphysis.
Fig. 2. Séries de reconstructions en 3D. Première ligne (a) : reconstructions effectuées avec VisualSFM ; deuxième ligne (b) : reconstructions effectuées avec Photoscan. Numéros des séries (dans l'ordre) : S1, S2, S3, S4, S5, S6. La flèche indique l'orientation de l'épiphyse proximale.

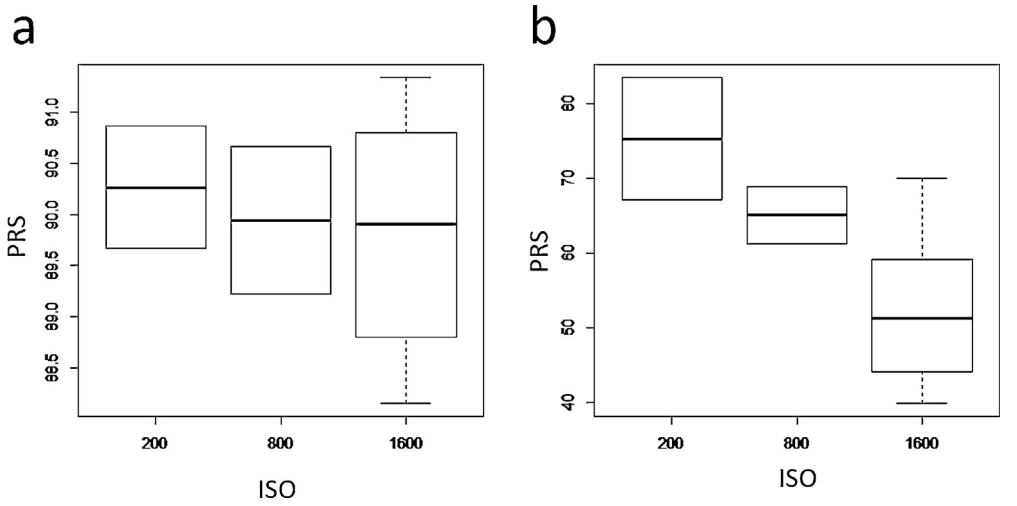

Fig. 3. Boxplots showing the Percentage of Reconstructed Surface (PRS) against the ISO value for all sets analyzed (except outdoors) for each software: a: with Photoscan; b: with VisualSFM.
Fig. 3. Graphiques en boîtes à moustache montrant le pourcentage de surface reconstruite en fonction de la valeur ISO pour chacune des séries (sauf celles prises en extérieur), pour les deux logiciels : a : Photoscan ; b : VisualSFM.

specimen was mounted because the contact areas were totally different, and the fact that the PRS values are very similar despite different conditions is probably a coincidence. However, the persistence of the difference between VisualSFM and Photoscan is interesting. Indeed, even with better light conditions, VisualSFM does not enable as good a 3D reconstruction as its commercial analog.

Moreover, the maximal PRS value with VisualSFM (83.4%; SF1) is below the minimal value with Photoscan (88.2%; SF5). In addition, the range (difference between the maximal and the minimal PRS value outdoor sets excluded) is very broad in VisualSFM (43.5%), and much narrower in Photoscan (3.2%). This is supported by the standard deviation (σ) values: $\sigma = 13.3$ and $\sigma = 1.1$, respectively (Fisher test, $P < 0.001$); the latter clearly shows that Photoscan is more regular than VisualSFM.

3.2. Influence of luminosity, photoflash and ISO parameter

No influence of the lighting condition (natural vs artificial added) could be observed in either program. Indeed, the mean PRS values for the sets with additional artificial light (S1, S3, S4, S7), which are 54.6% with VisualSFM and 90.0% with Photoscan, are not statistically different from those obtained in natural lighting conditions (S2, S5, S6, S8): 53.9% with VisualSFM and 90.3% with Photoscan (two-sample *t*-test: *P*-value = 0.944 for VisualSFM; *P*-value = 0.714 for Photoscan).

The use of pictures taken with photoflash did not improve the PRS in Photoscan (SF1, SF5 and SF6: mean PRS value = 89.2% versus 90.2% without photoflash), but there was an effect in VisualSFM: the mean PRS value of the sets with photoflash (SF6 = 61.0%, SF5 = 70.0%, SF1 = 83.4%) is clearly higher than without photoflash (lowest = 39.9%, mean = 54.3%, higher = 67.1%). However, due to the reduced sample size (8 sets against 3 without photoflash), this difference is not statistically significant at the threshold of 5% (Student test: $P = 0.094$), but there is a trend.

As for the camera's sensitivity, or ISO, it influences the PRS only with VisualSFM (Fig. 3). Indeed, there is no clear distinction in the PRS values between the different ISO values tested (200, 800 and 1600) with Photoscan (Fig. 3a). The fact that the range becomes bigger when ISO = 1600 is probably an artefact due to the bigger number of sets with this value (9 sets with 1600 ISO, 2 sets with 200 and 800 ISO, respectively). Conversely, when using VisualSFM, the PRS values tend to lower when the ISO values are higher (Fig. 3b).

3.3. Deviation analysis

The deviation analysis is expressed (in Geomagic Studio) with an encoded color scheme with a relative scale (Fig. 4). For all 3D models, most of the surface is colored in green, meaning that the distance between the 3D models and the RO is very small (approximately from −0.6 mm to 0.6 mm; each comparison has a unique relative scale). This shows that the 3D models obtained by photogrammetry are an effective and precise digital representation of the femur, given the fact that the specimen is mounted and non-displaceable. A Student test on the positive and negative deviation showed no statistical difference between the two software for the deviation analysis (Table 2; *t*-test: *P*-values = 0.5366 and 0.0563, respectively). Even outliers are in the same range for both programs (mean maximal deviation, see Table 2). Values of Mean deviation are all lower than 0.5 mm. Reported to the bone length that exceeded 40 cm, it shows that the quality of the reconstruction is precise enough to be used in quantitative studies (Fig. 4).

Maximal deviation values occur generally in the same areas (Fig. 4) that are those which were poorly lighted and/or difficult to access. In our setting, the knee joint

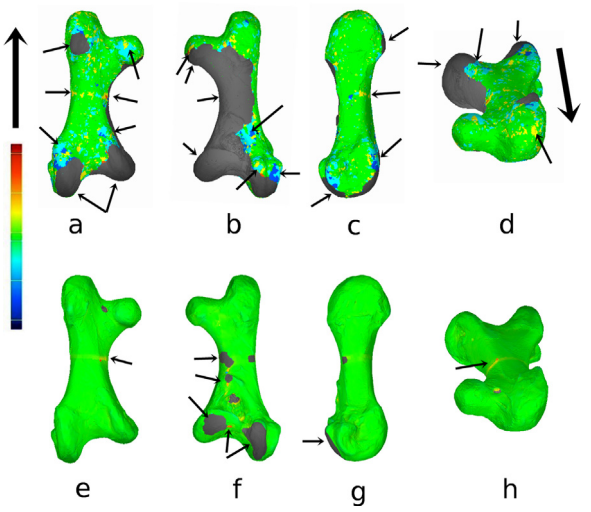

Fig. 4. Color representation of the deviation analysis. 3D models obtained by photogrammetry are compared to the RO (obtained with a surface scanner). Colored areas show the surface of the 3D model tested (S4), reconstructed with a–d: VisualSFM; e–h: Photoscan. Grey areas are those that were not reconstructed by photogrammetry (contact areas, and/or areas with poor luminosity); they thus correspond to the RO. The bigger arrow indicates the orientation of the proximal epiphysis, smaller arrows indicate areas with maximum of deviation or non-reconstructed. The color scale is relative and indicates the level of deviation; red: maximal positive deviation; green: no deviation; dark blue: maximal negative deviation. Views: a, e: dorsal; b, f: ventral; c, g: lateral; and d, h: femoral condylar joint.

Fig. 4. Représentation en couleur des distances entre la surface du modèle 3D (S4) reconstruit par photogrammétrie et l'objet de référence (RO) obtenu grâce à un scanner surfacique. Logiciel : a–d : VisualSFM ; e–h : Photoscan. La plus grande flèche indique l'orientation de l'épiphyse proximale, les plus petites flèches indiquent les zones où la distance entre les deux modèles est la plus grande, et les zones à déviation maximale ou non reconstruites. Les zones colorées représentent la surface obtenue par photogrammétrie, les zones grises correspondent aux zones non reconstruites (zones de contact et/ou zones de faible luminosité). L'échelle de couleur est relative et représente la distance entre les surfaces : rouge : distance maximale positive ; vert : pas de distance entre les deux surfaces ; bleu foncé : distance maximale négative. Vues : a, e : dorsale ; b, f : ventrale ; c, g : latérale ; et d, h : condyle fémoral.

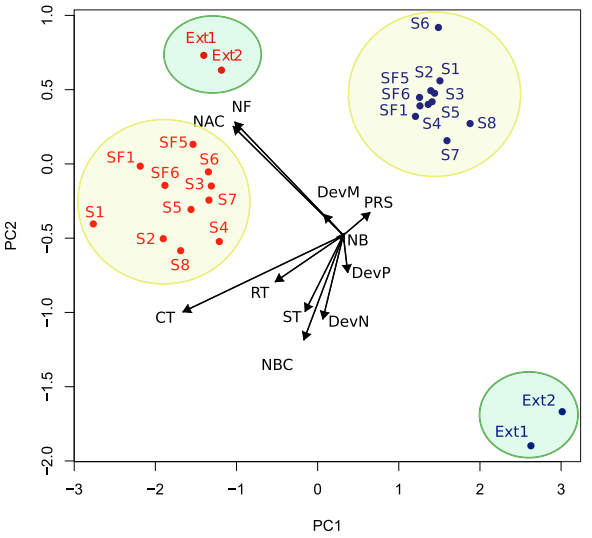

Fig. 5. Principal component analysis of quantitative data collected in this study. Red dots correspond to VisualSFM, and blue dots to Photoscan. Abbreviations: CT: Cleaning Time; DevM: maximum deviation; DevN: mean negative deviation; DevP: mean positive deviation; NAC: point number after cleaning; NB: number of photographs used for the "dense reconstruction"; NBC: point number before cleaning; NF: face number; PRS: Percentage of the Reconstructed Surface; RT: 3D Reconstruction Time; ST: standard deviation.

Fig. 5. Analyse en composantes principales des données quantitatives relevées lors de cette étude. Les points rouges correspondent aux reconstructions faites avec VisualSFM, les points bleus à celles faites avec Photoscan. Abréviations : CT : temps de nettoyage ; DevM : distance maximale entre les surfaces ; DevN : moyenne des distances négatives ; DevP : moyenne des distances positives ; NAC : nombre de points après nettoyage ; NB : nombre de photographies utilisées pour l'étape de « reconstruction dense » ; NBC : nombre de points avant nettoyage ; NF : nombre de faces ; PRS : pourcentage de surface reconstruite ; RT : temps de reconstruction 3D ; ST : écart-type.

was against the light. High deviation values occur in this area, as shown by the red and blue patches observable on Fig. 4a–d), meaning that the surface is not exactly the same as the surface of the RO. Areas against the light lead to very dark photographs difficult to manage for 3D reconstructions. Areas difficult to access were those where the femur is very close to a brace or to another bone, despite absence of contact (Fig. 4e–h). Naturally, contact areas cannot be reconstructed in any case.

3.4. Principal components analysis

The first two principal components (PC1 and PC2) concentrate 91.1% of the data variance, 79.5% and 11.5%, respectively. The PCA results are consistent with those previously obtained (Fig. 5). The PCA shows that the 3D models obtained mostly differ in terms of number of points (NAC, NF, NBC) and time of treatment (CT, RT). The PRS is not as important a factor as expected (based on our previous results), and it varies antagonistically to the cleaning time (CT). The choice of software clearly separates the sets on the first axis. 3D models obtained by Photoscan have higher PRS values than those from VisualSFM (as previously shown), and all the 3D models reconstructed with VisualSFM had required more time of treatment, notably cleaning time (CT), than those obtained with Photoscan. The second axis separates the outdoor sets from the others, but in opposite directions for each program. As a result, we can observe four different groupings on the PCA (Fig. 5). The sets are not separated by the photoflash, the ISO value, or the addition of artificial light. These parameters do not have a big effect on the 3D reconstruction, as seen previously. The fact that the outdoor sets are separated from the others shows that the proprieties of the 3D models obtained differ based on the environment, and not on the parameters previously tested. This means that each software is sensible to the environment (outdoor versus indoor) during the data acquisition, and it affects the quality and the time of treatment needed. All sets were clustered depending on the program used (four groups, Fig. 5), which shows that photogrammetry has a good repeatability for a given program and a given environment.

As VisualSFM does not take all the photographs during the "dense reconstruction" step, but eliminates photographs without enough matching points, the number

Table 2
Summary of the deviation analysis results between the 3D models obtained by photogrammetry and the reference object (RO). Deviation values in millimeters. Maximal deviation: maximal absolute distance between the same point on the tested 3D models and on the RO. Mean positive deviation: mean distance between the surface tested and the surface of the RO when the 3D model is above. The negative mean deviation is the same as the positive mean, but when the 3D model is below the RO surface.

Tableau 2
Résumé des analyses de distance entre les surfaces obtenues par photogrammétrie et l'objet de référence (RO). Distance en millimètres. *Maximal deviation* : distance absolue maximale entre deux points de surface homologues entre l'objet testé et le RO. *Mean positive deviation* : distance moyenne entre la surface testée et le RO lorsque la surface du RO est au-dessus de la surface testée. *Negative mean* : même chose que précédemment, mais lorsque la surface testée est au-dessous du RO.

	VisualSFM			Photoscan		
Sets	Maximal	Positive mean	Negative mean	Maximal	Positive mean	Negative mean
S1	17.599	0.466	−0.713	12.791	0.431	−0.304
S2	17.599	0.416	−0.564	11.095	0.356	−0.313
S3	17.594	0.266	−0.413	17.585	0.431	−0.457
S4	17.591	0.375	−0.612	16.562	0.372	−0.309
S5	17.599	0.322	−0.481	13.584	0.415	−0.276
S6	17.557	0.401	−0.475	16.804	0.264	−0.198
S7	17.598	0.502	−0.456	10.724	0.416	−0.326
S8	17.6	0.426	−0.529	11.001	0.339	−0.336
SF1	17.596	0.415	−0.543	17.587	0.375	−0.409
SF5	17.584	0.318	−0.332	19.931	0.341	−0.266
SF6	17.599	0.317	−0.406	13.574	0.343	−0.236
Sext1	18.136	0.179	−0.229	9.163	0.45	−0.534
Sext2	18.096	0.222	−0.199	12.972	0.379	−0.377
Mean	17.673	0.356	−0.458	14.106	0.378	−0.334

of photographs used for the dense reconstruction (NB) changes depending on the set used (e.g., SF1: NB = 223; S7: NB = 245). This is not a source of variation here (Fig. 5). The number of points before cleaning (NBC) and the number of points after cleaning (NAC), conversely, are an important source of variation, in almost perpendicular directions. A high NBC is thus not synonymous with a high NAC. Likewise, the NAC goes in a perpendicular direction to the PRS, showing that a high NAC does not necessarily mean a more complete 3D model. Deviation (DevM, DevN, DevP) and PRS are not important factors on the set distribution as compared to NAC (and NF that is correlated to NAC: one face being a triangular surface made with 3 points), NBC and CT. This clearly shows that the quality of a 3D model is not proportional to the time spent on it.

4. Discussion

Our results show that the surfaces reconstructed by photogrammetry are very close to those produced by the resort to a cutting-edge surface scanner. But there is a big difference between the commercial and the open source software tested here, both being voluntarily used with their default parameters. Photoscan (the commercial one) is more effective than VisualSFM, since the 3D models produced are much more complete. This remains true whatever the brightness conditions, as shown by the fact that both indoor and outdoor VisualSFM (using CMVS tool) reconstructions were not as effective as Photoscan's. Therefore, in similar conditions, Photoscan was always the most effective. One possible explanation is that VisualSFM is more sensitive to the lack of light than Photoscan. VisualSFM seems also to be more sensitive to the ISO value, as the PRS declined when the ISO increased. This can probably be explained by the increase of numeric noise that, interfering with the reconstruction algorithm in VisualSFM (CMVS), decreases the ability to find matching points and leads to not obtain an optimal PRS. However, the performances discussed are based on reconstructions performed with default parameters. 3D models presented here are not the best that can be obtained by either program in the present conditions, because, though the default parameters are the most polyvalent, it is possible to improve the quality of the 3D models by adapting the camera and reconstruction parameters. A good knowledge of programming, in photography and/or in photogrammetry might allow one to obtain better results with both programs. But finding matching points on cameras can also be a specific issue of VisualSFM, as a recent comparison between this programs and the web service ARC3D (www.arc3d.be) showed that 3D models obtained with VisualSFM were less complete than those obtained with ARC3D (Cipriani et al., 2016). The light cannot be a limited element because Cipriani et al. (2016) tried to digitize a small geological outcrop; the performance of VisualSFM is thus directly challenged in the paper.

The 3D models we obtained with VisualSFM are not suitable for scientific study. Photoscan, beyond its higher performance, is also easier to use for beginners, and faster. The present study shows that Photogrammetry is a method of 3D data acquisition of mounted and exposed skeleton suitable for quantitative analyses. But as in Bevan et al. (2014), it is possible to use both programs, or even additional programs not tested here, and then only retain the best 3D model for study. Moreover, as Mallison and Wings (2014) highlighted, we strongly recommend that users adapt protocols (e.g., parameters of the camera and program, number of photographs) to each situation they will face, and not only work using the default or automatic parameter in order to obtain 3D models of the best possible quality.

Photoscan offers many possibilities that have not been tested here, and even the mesh surface generation is possible (here we used Geomagic Studio to generate the mesh

surface). At least, one of the simplest methods to improve the 3D model produced is to choose a higher level of detail, as Photoscan proposes several levels of detail (lowest, low, medium, high, and ultra-high) at the beginning of each step of the reconstruction process (photo alignment, 3D reconstruction, and mesh building). The quality of the surface produced in terms of detailed color and topology fidelity, and the total time of processing fluctuates depending on the level of detail chosen (Koutsoudis et al., 2014). The higher the level of detail, the higher the precision of the 3D model. Koutsoudis et al. (2014) showed that a 3D reconstruction having about 1 million vertices (number of points) with the lowest option, displayed more than 161 million vertices with the highest one. The time of processing fluctuates similarly from 16 minutes to more than 17 hours. We can expect a higher precision in the areas of highest deviation, and thus a more complete 3D model in the limits of the possible (contact with braces and bones) with a higher level of detail. If the main purpose is to reconstruct the maximum of bone's surface, it is not always necessary to choose the higher reconstruction option because the gain of surface could be disappointing compared to the time required. We tried the "high" option in Photoscan for the set S6, and we obtained a 3D model with NAC (Number of points After Cleaning) = 2,501,823, and PRS = 92.02% after about 7 hours of treatments, against NAC = 521,398, PRS = 91.33% and less than 1 hour of treatments for the 3D model with the "lowest" option. The high option is more accurate, with more details and a more complex surface, but there is not a great difference in the PRS, and no visible improvement of the areas always reconstructed with the lowest option. So, the options have to be chosen based on the purpose, e.g., if it the shape of the bones or an accurate surface that is needed. The high and ultra-high options are very time consuming, and not always useful, because as we show here, the lowest option is often sufficient to get an accurate and almost complete 3D model. This is also relevant for the resolution of the camera and its impact on the 3D reconstruction, because the principle of the reconstruction option in Photoscan is to reduce the resolution (number of pixels) of the photographs. According to Falkingham (2012), processing time and memory needed increase exponentially with the resolution. As for the reconstruction option, we discussed previously, the camera with the higher resolution is not always the best choice. A resolution range between 8 and 12 mega-pixels seems a perfectly suitable choice.

Moreover, our study showed that the 3D models with the highest number of points or which had taken the longest reconstruction time are not necessarily the ones with the best quality. Models with Photoscan were better than with VisualSFM, though the reconstructions were quicker and the 3D models had less points than with VisualSFM (see Appendix 1). This is not just a software issue. When comparing two 3D models obtained with Photoscan, we cannot see a correlation between the NBC (Number of points Before Cleaning), NAC and PRS. For example, the set S8: NBC = 1,216,423, NAC = 373,887, and PRS = 90.7%, and SF1: NBC = 1,245,699, NAC = 504,307, PRS = 89.7%. This seems to indicate that: (1) the NBC cannot predict the NAC; (2) the NAC cannot predict the PRS.

As seen with the PCA, there is no linear relationship between these three variables. As a consequence, it can be useless to try to increase the number of points (NBC and NAC) of a 3D model in order to improve the PRS. As seen previously, a higher option in reconstruction parameter, albeit providing more points (higher NBC and NAC) is not synonymous of more surface reconstructed (PRS).

5. Conclusion

Photogrammetry is a lot cheaper than other currently used 3D data acquisition methods. Moreover, it has the important advantage of being mobile and can thus be used anywhere (Cunningham et al., 2014). In paleontology, many large specimens are mounted and displayed in museum galleries. Photogrammetry appears a well-adapted method to digitize such specimens. However, in museum galleries, the lack of light can be problematic as it is a limiting element, since bad light exposure is fatal for the quality of photographs. Our study interestingly showed high quality results with the use of the commercial software Agisoft Photoscan even in limited light conditions. The 3D models produced are of comparable quality to those produced with a high quality surface scanner. Only areas in contact with other bones or with braces caused by mounting cannot be reconstructed here. It confirms that photogrammetry, rather underused in paleontology, is a reliable method for quantitative analyses (as previously suggested by Falkingham, 2012; Petti et al., 2008; Remondino et al., 2010). But, especially, it shows that photogrammetry is a very adequate method to digitize bones of mounted specimens. Nevertheless, it must not be forgotten that the quality of the 3D reconstruction with photogrammetry relies on the materials used (camera and software). As these two programs (i.e. VisualSFM and Agisoft Photoscan) were only used in this study with their default parameters, we do not state that one is better than the other, but only that Photoscan is easier to use for an unaccustomed user, and that the 3D models obtained are suitable for quantitative studies. Photogrammetry is still underused in 3D paleontology, and all the possibilities and options that this method can bring to the field remain to be further explored.

Acknowledgments

We are grateful to Allowen Evin (MNHN, Paris, France) for discussions and suggestions, Vincent Pernègre and Ronan Allain (MNHN) for making the specimen of *Aepyornis* available for study, and Léo Botton-Divet (MNHN) for his precious help with the surface scanner. We thank the Morphometric platform of the "Muséum national d'histoire naturelle" (UMS 2700 CNRS/MNHN "Outils et méthodes de la systématique intégrative") for providing access. We are particularly grateful to Lilian Cazes (MNHN), for his fruitful advices, notably regarding the use of the software. We particularly thank Peter Falkingham (Liverpool John Moores University, UK) and the two anonymous reviewers, whose comments helped us improve the quality of this paper, and also Kevin Padian (UCB) for his proof reading and helpful suggestions. A.H. acknowledges financial support from the ANR-13-PDOC-0011.

Appendix A. Supplementary data

Supplementary data associated with this article can be found, in the online version, at http://dx.doi.org/10.1016/j.crpv.2016.08.003.

References

Bartoš, K., Pukanská, K., Sabová, J., 2014. Overview of available open-source photogrammetric software, its use and analysis. Int. J. Innov. Educ. Res. 2, 62–70.

Belvedere, M., Jalil, N.-E., Breda, A., Gattolin, G., Bourget, H., Khaldoune, F., Dyke, G.J., 2013. Vertebrate footprints from the Kem Kem beds (Morocco): A novel ichnological approach to faunal reconstruction. Palaeogeogr. Palaeoclimatol. Palaeoecol., 383–384, http://dx.doi.org/10.1016/j.palaeo.2013.04.026 [52–8].

Bevan, A., Li, X., Martinón-Torres, M., Green, S., Xia, Y., Zhao, K., Zhao, Z., Ma, S., Cao, W., Rehren, T., 2014. Computer vision, archaeological classification and China's terracotta warriors. J. Archaeol. Sci. 49, 249–254, http://dx.doi.org/10.1016/j.jas.2014.05.014.

Bonneau, N., Libourel, P.-A., Simonis, C., Puymerail, L., Baylac, M., Tardieu, C., Gagey, O., 2012. A three-dimensional axis for the study of femoral neck orientation. J. Anat. 221, 465–476, http://dx.doi.org/10.1111/j.1469-7580.2012.01565.x.

Brassey, C.A., Maidment, S.C.R., Barrett, P.M., 2015. Body mass estimates of an exceptionally complete *Stegosaurus* (Ornithischia: Thyreophora): comparing volumetric and linear bivariate mass estimation methods. Biol. Lett. 11, 20140984, http://dx.doi.org/10.1098/rsbl.2014.0984.

Breithaupt, B.H., Matthews, N.A., 2001. Preserving paleontological resources using photogrammetry and geographic information systems. In: Crossing Boundaries in Park Management, Proceedings of the 11th Conference on Research and Resource Management in Parks and Public Lands. The George Wright Society, Inc.

Breithaupt, B.H., Southwell, E.H., Adams, T., Matthews, N.A., 2001. Innovative documentation methodologies in the study of the most extensive dinosaur tracksite in Wyoming. In: 6th Fossil Research Conference Proceedings Volume, pp. 113–122.

Breithaupt, B.H., Matthews, N.A., Noble, T.A., 2004. An integrated approach to three-dimensional data collection at dinosaur tracksites in the Rocky Mountain West. Ichnos 11 (1–2), 11–26.

Castanera, D., Pascual, C., Razzolini, N.L., Vila, B., Barco, J.L., Canudo, J.I., 2013. Discriminating between Medium-Sized Tridactyl Trackmakers: Tracking Ornithopod Tracks in the Base of the Cretaceous (Berriasian, Spain). PLoS ONE 8, e81830, http://dx.doi.org/10.1371/journal.pone.0081830.

Cipriani, A., Citton, P., Romano, M., Fabbi, S., 2016. Testing two open-source photogrammetry software as a tool to digitally preserve and objectively communicate significant geological data: the Agolla case study (Umbria-Marche Apennines). Ital. J. Geosci. 135, 199–209.

Clarac, F., Souter, T., Cornette, R., Cubo, J., de Buffrénil, V., 2015. A quantitative assessment of bone area increase due to ornamentation in the Crocodylia. J. Morphol. 276, 1183–1192, http://dx.doi.org/10.1002/jmor.20408.

Cunningham, J.A., Rahman, I.A., Lautenschlager, S., Rayfield, E.J., Donoghue, P.C., 2014. A virtual world of paleontology. Trends Ecol. Evol. 29, 347–357, http://dx.doi.org/10.1016/j.tree.2014.04.004.

De Reu, J., De Smedt, P., Herremans, D., Van Meirvenne, M., Laloo, P., De Clercq, W., 2014. On introducing an image-based 3D reconstruction method in archaeological excavation practice. J. Archaeol. Sci. 41, 251–262, http://dx.doi.org/10.1016/j.jas.2013.08.020.

De Reu, J., Plets, G., Verhoeven, G., De Smedt, P., Bats, M., Cherretté, B., De Maeyer, W., Deconynck, J., Herremans, D., Laloo, P., Van Meirvenne, M., De Clercq, W., 2013. Towards a three-dimensional cost-effective registration of the archaeological heritage. J. Archaeol. Sci. 40, 1108–1121, http://dx.doi.org/10.1016/j.jas.2012.08.040.

Fabre, A.C., Cornette, R., Goswami, A., Peigné, S., 2015. Do constraints associated with the locomotor habitat drive the evolution of forelimb shape? A case study in musteloid carnivorans. J. Anat. 226, 596–610, http://dx.doi.org/10.1111/joa.12315.

Falkingham, P.L., 2012. Acquisition of high resolution three-dimensional models using free, open-source, photogrammetric software. Palaeontol. Electron. 15, 15.

Falkingham, P.L., 2013. Generating a photogrammetric model using Visual SFM and post-processing with meshlab. Brown University, Tech. Rep.

Furukawa, Y., Ponce, J., 2010. Accurate, dense, and robust multiview stereopsis. Pattern Anal. Mach. Intell. IEEE Trans. On 32, 1362–1376.

Guarnieri, A., Remondino, F., Vettore, A., 2004. Photogrammetry and Ground-based Laser Scanning: Assessment of Metric Accuracy of the 3D Model of Pozzoveggiani Church. In: FIG Working Week 2004. TS on "Positioning and Measurement Technologies and Practices II-Laser Scanning and Photogrammetry.

Hutchinson, J.R., Anderson, F.C., Blemker, S.S., Delp, S.L., 2005. Analysis of hindlimb muscle moment arms in *Tyrannosaurus rex* using a three-dimensional musculoskeletal computer model: implications for stance, gait, and speed. Paleobiology 31, 676–701, http://dx.doi.org/10.1666/0094-8373(2005)031 [0676:AOHMMA]2.0.CO;2.

Jiang, R., Jáuregui, D.V., White, K.R., 2008. Close-range photogrammetry applications in bridge measurement: literature review. Measurement 41, 823–834, http://dx.doi.org/10.1016/j.measurement.2007.12.005.

Koutsoudis, A., Vidmar, B., Arnaoutoglou, F., 2013. Performance evaluation of a multi-image 3D reconstruction software on a low-feature artefact. J. Archaeol. Sci. 40, 4450–4456, http://dx.doi.org/10.1016/j.jas.2013.07.007.

Koutsoudis, A., Vidmar, B., Ioannakis, G., Arnaoutoglou, F., Pavlidis, G., Chamzas, C., 2014. Multi-image 3D reconstruction data evaluation. J. Cult. Herit. 15, 73–79, http://dx.doi.org/10.1016/j.culher.2012.12.003.

Laloy, F., Rage, J.C., Evans, S.E., Boistel, R., Lenoir, N., Laurin, M., 2013. A Re-Interpretation of the Eocene Anuran *Thaumastosaurus* Based on MicroCT Examination of a "Mummified" Specimen. PLoS ONE 8, e74874, http://dx.doi.org/10.1371/journal.pone.0074874.

Lane, S.N., James, T.D., Crowell, M.D., 2000. Application of Digital Photogrammetry to Complex Topography for Geomorphological Research. Photogramm. Rec. 16, 793–821, http://dx.doi.org/10.1111/0031-868X.00152.

Mallison, H., Wings, O., 2014. Photogrammetry in paleontology – a practical guide. J. Paleontol. Techniques 12, 1–31.

Matthews, N.A., Breithaupt, B.H., 2001. Close Range Photogrammetric Experiments at Dinosaur Ridge. Mountain Geol. 38 (3), 147–154.

Mora, P., Baldi, P., Casula, G., Fabris, M., Ghirotti, M., Mazzini, E., Pesci, A., 2003. Global Positioning Systems and digital photogrammetry for the monitoring of mass movements: application to the Ca'di Malta landslide (northern Apennines, Italy). Eng. Geol. 68, 103–121, http://dx.doi.org/10.1016/S0013-7952(02)00200.

Petti, F.M., Avanzini, M., Belvedere, M., De Gasperi, M., Ferretti, P., Girardi, S., Remondino, F., Tomasoni, R., 2008. Digital 3D modelling of dinosaur footprints by photogrammetry and laser scanning techniques: integrated approach at the Coste dell'Anglone tracksite (Lower Jurassic, southern Alps, northern Italy). Studi Trentini Sci. Nat. Acta Geol. 83, 303–315.

Polly, P.D., Lawing, A.M., Fabre, A.-C., Goswami, A., 2013. Phylogenetic principal components analysis and geometric morphometrics. Hystrix Ital. J. Mammal. 24, 33–41.

Pradel, A., Langer, M., Maisey, J.G., Geffard-Kuriyama, D., Cloetens, P., Janvier, P., Tafforeau, P., 2009. Skull and brain of a 300-million-year-old chimaeroid fish revealed by synchrotron holotomography. Proc. Proc. Natl. Acad. Sci. 106, 5224–5228, http://dx.doi.org/10.1073/pnas.0807047106.

Rahman, I.A., Smith, S.Y., 2014. Virtual paleontology: computer-aided analysis of fossil form and function. J. Paleontol. 88, 633–635, http://dx.doi.org/10.1666/13-001I.

Remondino, F., Rizzi, A., Girardi, S., Petti, F.M., Avanzini, M., 2010. 3D Ichnology-recovering digital 3D models of dinosaur footprints. Photogramm. Rec. 25, 266–282, http://dx.doi.org/10.1111/j.1477-9730.2010.00587.x.

Rücklin, M., Donoghue, P.C.J., Cunningham, J.A., Marone, F., Stampanoni, M., 2014. Developmental paleobiology of the vertebrate skeleton. J. Paleontol. 88, 676–683, http://dx.doi.org/10.1666/13-107.

Salonia, P., Bellucci, V., Scolastico, S., Marcolongo, M., Leti Messina, T., 2007. 3D survey technologies for reconstruction, analysis and diagnosis in the conservation process of cultural heritage. In: Proceedings of The 21st CIPA symposium 2007.

Salonia, P., Leti Messina, T., Marcolongo, A., Scolastico, S., 2009. Three focal photogrammetry application for multi-scale and multi-level Cultural Heritage survey, documentation and 3D reconstruction. In: Proceedings of The 22nd CIPA Symposium 2009.

Warne, M., 2015. Photogrammetric software as an alternative to 3D laser scanning in an amateur environment. Degree project in media technology, second level, Cracow. Univerity of Technology, Stockholm, Sweden.

Wolf, P.R., Dewin, B.A., 2000. Elements of Photogrammetry with application in GIS, 3. McGraw Hill, New York [624 p.].

Wu, C., 2011. VisualSFM: A visual structure from motion system. http://ccwu.me/vsfm/.

Wu, C., Agarwal, S., Curless, B., Seitz, S.M., 2011. Multicore bundle adjustment. In: Computer Vision and Pattern Recognition (CVPR), 2011 IEEE Conference on IEEE (pp. 3057-3064).